



HAL
open science

Predicting chaotic time series using optoelectronic feedback laser

Pavel S Dmitriev, Anton V Kovalev, A. Locquet, David S Citrin, Evgeny A Viktorov, Damien Rontani

► **To cite this version:**

Pavel S Dmitriev, Anton V Kovalev, A. Locquet, David S Citrin, Evgeny A Viktorov, et al.. Predicting chaotic time series using optoelectronic feedback laser. *Semiconductor Lasers and Laser Dynamics IX*, Apr 2020, Online Only, France. pp.32, 10.1117/12.2556368 . hal-03084699

HAL Id: hal-03084699

<https://hal.science/hal-03084699v1>

Submitted on 21 Dec 2020

HAL is a multi-disciplinary open access archive for the deposit and dissemination of scientific research documents, whether they are published or not. The documents may come from teaching and research institutions in France or abroad, or from public or private research centers.

L'archive ouverte pluridisciplinaire **HAL**, est destinée au dépôt et à la diffusion de documents scientifiques de niveau recherche, publiés ou non, émanant des établissements d'enseignement et de recherche français ou étrangers, des laboratoires publics ou privés.

Predicting chaotic time series using optoelectronic feedback laser

Pavel S. Dmitriev^a, Anton V. Kovalev^a, Alexandre Locquet^{b,c}, David S. Citrin^{b,c}, Evgeny A. Viktorov^a, and Damien Rontani^d

^aITMO University, Birzhevaya Liniya 14, Saint Petersburg, Russia

^bGeorgia Tech-CNRS UMI 2958, Georgia Tech Lorraine, 2 Rue Marconi, 57070 Metz, France

^cSchool of Electrical and Computer Engineering, Georgia Institute of Technology, Atlanta, Georgia 30332-0250, USA

^dLMOPS EA 4423 Laboratory, Universite de Lorraine & CentraleSupélec, 2 rue Edouard Belin, F-57070 Metz, France

ABSTRACT

We study delay-based photonic reservoir computing using a semiconductor laser with an optoelectronic feedback. A rate-equation model for a laser with an optoelectronic filtered feedback is used. The filter allows only high-frequency signals to pass through the feedback loop. The delay-differential equation model consists of three equations for the normalized electric field intensity, the carrier density, and the filtered intensity signal. The stability boundaries which correspond to the Hopf bifurcation condition are determined analytically, showing multiple Hopf bifurcation branches in the dynamics, and the parity asymmetry with relation to the feedback sign. We use the Santa Fe time-series prediction task to evaluate the performance of reservoir computing. Our objective is to determine location of the optimal operating point defined as corresponding to minimal normalized mean square error (NMSE) and relate it to the stability properties of the system. We use 3000 points for training and 1000 for testing; the number of virtual nodes is chosen in regard to the relaxation oscillation frequency. The input signal is determined by the chaotic waveform having n sampling points, and three cases are investigated prediction of $n + 1$, $n + 2$ or $n + 3$ sampling point. The minimum values of NMSE for the $n + 2$ and $n + 3$ point prediction tasks correspond to the Hopf bifurcation, and only for the positive feedback.

Keywords: reservoir computing, semiconductor laser, optoelectronic feedback, bifurcation analysis

1. INTRODUCTION

As conventional computer architectures are approaching their limit, there is an upsurge of research devoted to finding new efficient and fast ways of data processing. Photonic reservoir computing (RC) is a promising paradigm combining the computational capabilities of recurrent neural networks with high processing speed and energy efficiency of photonics. The principle of operation of photonic RC systems lies on the capability of nonlinear dynamical photonic systems to map an input signal onto a high-dimensional space allowing for the utilization of simple regression methods to solve complex time-series prediction and classification tasks. Generally, a recurrent network is used as a reservoir due to having fading memory. A single nonlinear system subject to a time-delayed feedback can be considered as a virtual network, and the internal states of virtual nodes are assigned by sampling the temporal waveform of the dynamical output within the feedback loop. This allows for easy hardware implementation of the virtual network exploiting a single nonlinear dynamical system with a time-delayed feedback loop. Many studies have been reported on the implementation of delay-based reservoir computing using optical and photonic systems, such as optoelectronic systems, all-optical systems, and laser dynamical systems.¹⁻³ In particular, semiconductor lasers with time-delayed feedback are very promising for the high-speed implementation of reservoir computing over gigahertz, owing to their fast relaxation oscillation frequencies. To enrich the distinctive properties of the reservoir, laser system is expected to operate close to

Further author information: (Send correspondence to A.V.K.)

A.V.K.: E-mail: avkovalel@niuitmo.ru

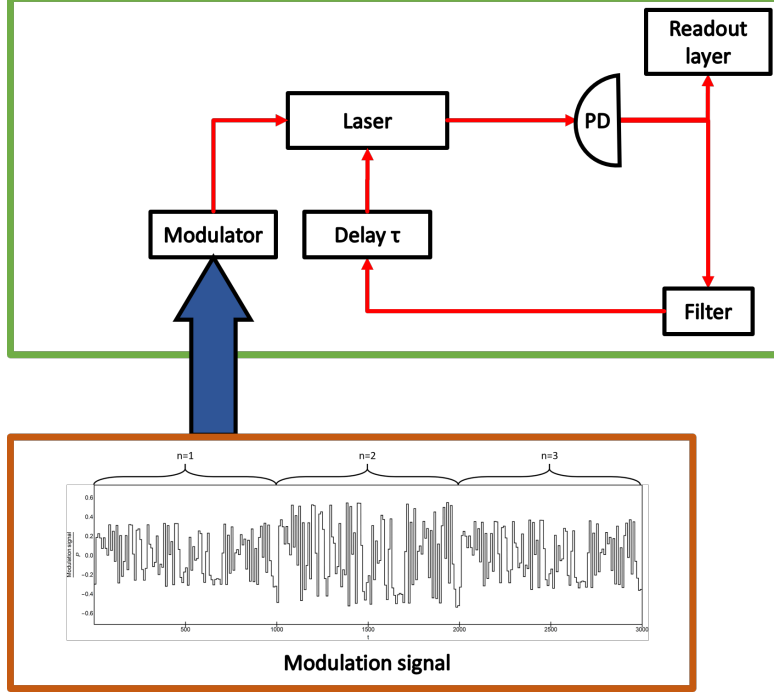


Figure 1. Schematic of the proposed optical reservoir computing system based on a laser with low-cut filtered optoelectronic feedback and the modulation signal.

a bifurcation point. We study delay-based photonic reservoir computing using a semiconductor laser with an optoelectronic feedback. Rate equation model for a laser with an optoelectronic filtered feedback is used. The filter allows only high-frequency signals to pass through the feedback loop. The stability boundaries which correspond to the Hopf bifurcation condition are determined analytically, showing multiple Hopf bifurcation branches in the dynamics, and parity asymmetry with relation to the feedback sign. We use the Santa Fe time-series prediction task⁴ to evaluate the performance of reservoir computing. Our objective is to determine the location of the optimal operating point defined as a point with minimal normalized means square error (NMSE) and relate it to the stability properties of the system.

2. THEORETICAL MODEL

Schematic of the proposed optical reservoir computing system based on a laser with low-cut filtered optoelectronic feedback is shown in Fig. 1.

For delay-based photonic reservoir computing, we explore the delay differential equation model for a laser with optoelectronic feedback having a low-cut filter in a feedback loop which reads as follows:^{5,6}

$$\dot{I}(t) = 2N(t)I(t), \quad (1)$$

$$\dot{I}_F(t) = -\tau_F^{-1}I_F(t) + 2N(t)I(t), \quad (2)$$

$$\begin{aligned} \varepsilon^{-1}\dot{N}(t) &= P + \eta I_F(t - \tau) - N(t) \\ &\quad - (1 + 2N(t))I(t), \end{aligned} \quad (3)$$

where the dot means differentiation with respect to $t \equiv \hat{t}/\tau_{ph}$ where \hat{t} is time, and τ_{ph} is the photon lifetime. $P = J/J_{th} - 1$ is the pump above the threshold parameter; η is the feedback strength; τ is the feedback delay; ε is the ratio of the carrier and photon lifetimes; τ_F^{-1} is the low-cut (high-pass) filter bandwidth.

Unlike the case of optical feedback, which has been examined in various RC systems, there is a single non-zero intensity steady state ($I = P$, $I_F = 0$, $N = 0$) in the case of a laser with optoelectronic feedback described by

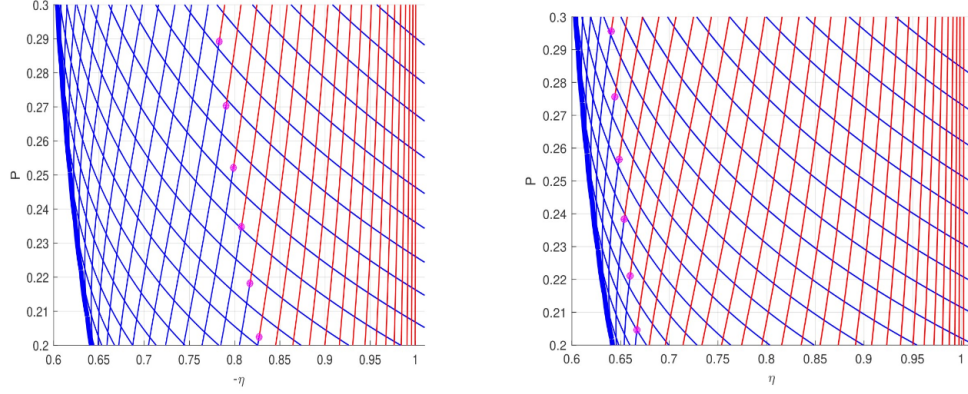


Figure 2. Hopf bifurcation boundaries in the (η, P) parameter plane calculated from Eqs. (5)–(7) for the negative (left panel) and positive (right panel) feedback. The blue (red) lines correspond to the supercritical (subcritical) Hopf bifurcation of the steady state; the circles are the generalized Hopf bifurcation points. The other parameters are: $\varepsilon = 0.1$, $\tau = 1000$, $\tau_F = 2000$. The bold lines correspond to the first Hopf bifurcation of the steady state.

Eqs. (1)–(3). The characteristic equation from the linearized Eqs. (1)–(3) reads:

$$(1 + \tau_F \lambda) \{ \lambda^2 + \varepsilon(\lambda + 2P(1 + \lambda)) \} - 2\varepsilon\eta\tau_F P \lambda e^{-\tau\lambda} = 0. \quad (4)$$

We are interested in the stability boundaries which correspond to the Hopf bifurcation condition $\lambda = \pm i\omega_H$. The Hopf frequency ω_H can be determined from the transcendental equation:

$$\arctan \frac{(1 + 2P(1 + \tau_F))\varepsilon\omega_H - \tau_F\omega_H^3}{(1 + \varepsilon\tau_F(1 + 2P))\omega_H^2 - 2\varepsilon P} = \omega_H\tau + \frac{\pi}{2} - \pi M, \quad (5)$$

$$\arctan \frac{(1 + 2P)\varepsilon\omega_H}{\omega_H^2 - 2\varepsilon P} = \omega_H\tau + \frac{\pi}{2} - \pi M, \quad (6)$$

where M is a non-negative integer number and is odd for negative feedback ($\eta < 0$), and is even for positive feedback ($\eta > 0$). Various M correspond to multiple Hopf bifurcation branches and indicate the discretization of the frequencies in Eq. (5) which is also parity-asymmetric with respect to the feedback sign since different resonant conditions formed by the parity of M .

The Hopf bifurcation point η_H is expressed analytically,

$$\eta_H = \frac{\varepsilon + 2\varepsilon P(1 + \tau_F) - \tau_F\omega_H^2}{2\varepsilon\tau_F P \cos \omega_H\tau}. \quad (7)$$

and is also parity-asymmetric due to $\cos \omega_H\tau$ term.

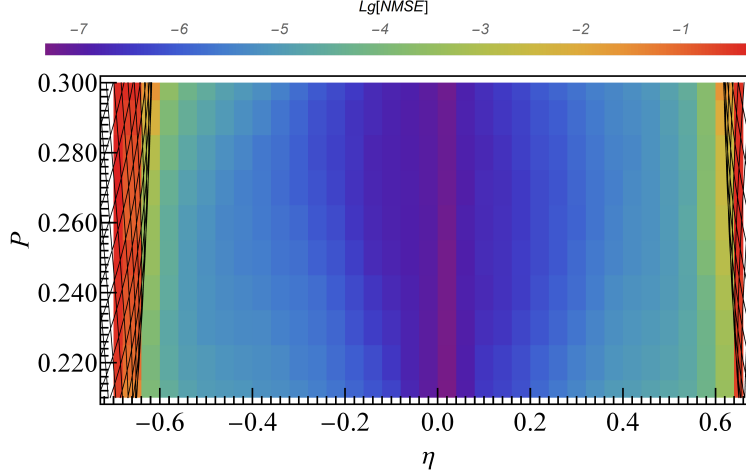


Figure 3. Color denotes $\lg(NMSE)$ in the case of $n + 1$ prediction task in (η, P) plane. Black lines correspond to the Hopf bifurcation branches. The other parameters are: $\varepsilon = 0.1$, $\tau = 1000$, $\tau_F = 2000$.

In the long delay limit $\tau \gg 1$ and the small filter bandwidth $\tau_F^{-1} \rightarrow 0$. Eqs. (5)–(7) can be approximated

$$\omega_H = \sqrt{\omega_{RO}^2 - \gamma_{RO}^2}, \quad (8)$$

$$\eta_H = \pm \frac{\gamma_{RO}\omega_{RO}}{\varepsilon P}, \quad (9)$$

where $\omega_{RO} \equiv \frac{1}{2}\sqrt{8\varepsilon P - \varepsilon^2(1 + 2P)^2}$ is the RO angular frequency of the free-running laser ($\eta = 0$), and $\gamma_{RO} \equiv \frac{1}{2}\varepsilon(1 + 2P)$ is RO damping rate.⁵ The bifurcation border in this limit is symmetric with respect to the sign of η which is not the case when the filtering is absent from the system (*i.e.*, $I_F(t) = I(t)$) because then the steady state intensity depends on η . Fig. 2 shows the Hopf bifurcation curves in the (η, P) parameter plane obtained by solving Eqs. (1)–(3). The sub-/supercritical parts and generalized Hopf points were determined by numerical package DDE-Biftool.⁷

3. RESERVOIR COMPUTING: INITIAL CONDITIONS

We use the Santa Fe time-series prediction task to evaluate the performance of reservoir computing. Our objective is to determine the location of the optimal operating point in (η, P) plane defined as a point with minimal normalized mean square error (NMSE) and relate it to the stability properties of the system. We use 3000 points for training and 1000 for testing; the number of virtual nodes is chosen in order to match the relaxation oscillation frequency. Input signal is determined by the chaotic waveform having n sampling points, and three cases are investigated: prediction of $n + 1$, $n + 2$ or $n + 3$ sampling point. For each pair of (η, P) the system started from stable lasing state $(P, 0, 0)$, and 4000 data points multiplied by random mask were used to modulate the P parameter. The generic modulation signal is shown in Fig. 1. The laser output signal is detected by the photodiode and amplified. The electronic signal is low-cut filtered in the feedback loop due to the bandwidth limitations of the photodiode and amplifier. This signal is added to (positive feedback) or subtracted from (negative feedback) the pump current driving the laser. Feeding the input data to the reservoir is performed by modulating the pump current. Finally, a white-noise term was added to Eqs. (1)–(3) to model the sponatenous emission. The modulation signal derived from multiplication of the input data by the mask. Result of the reservoir computing is determined by the multiplication of the intensity values at the virtual nodes by the weights implemented at the readout layer.

4. RESERVOIR COMPUTING: PREDICTION OF $N + 1$ OR $N + 3$ SAMPLING POINT

Let us firstly consider the case of $n + 1$ prediction task. The obtained result is shown in Fig. 3. The best value of NMSE (about 10^{-7}) is obtained in the absence of feedback; this can be explained by the simplicity of the task.

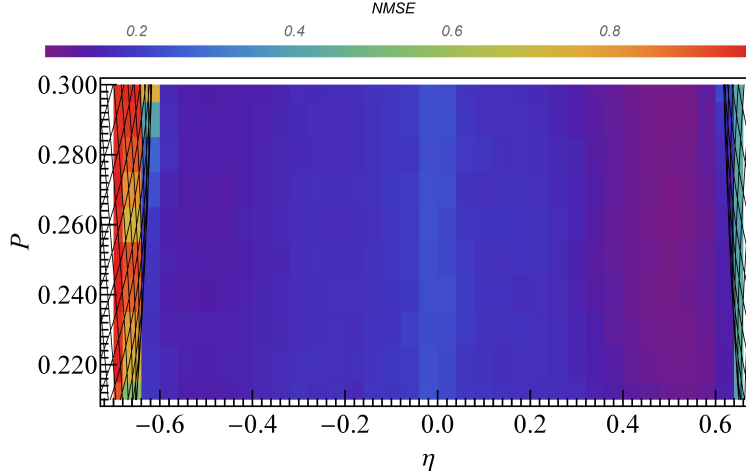


Figure 4. Color denotes $\lg(NMSE)$ in the case of $n + 3$ prediction task in (η, P) plane. Black lines correspond to the Hopf bifurcation branches. The other parameters are: $\varepsilon = 0.1$, $\tau = 1000$, $\tau_F = 2000$.

The dramatic increase in the NMSE values starts at the Hopf bifurcation boundary.

For the case of $n + 2$ and $n + 3$ prediction tasks, the optimal conditions determined by NMSEs in (η, P) plane change dramatically as shown in Fig. 4 for $n + 3$ prediction task. $\eta = 0$ or the absence of the feedback is now the worst in terms of NMSE, and the minimal NMSEs are moving close to the Hopf bifurcation boundary. There is also explicit asymmetry in Fig. 4 as optimal condition is demonstrated for positive feedback.

Fig. 5 shows the temporal waveforms of the input signal and the output of the response laser in the absence of the feedback ($\eta = 0$) which is optimal for $n + 1$ prediction task and close to the bifurcation boundary $\eta = 0.6$ which is optimal for $n + 2$ or $n + 3$ prediction tasks. The error signal between the original signal and the prediction signal based on a laser with optoelectronic low-cut filtered feedback is much stronger for $\eta = 0.6$, but we found that the reservoir computing for $n + 2$ or $n + 3$ prediction tasks at $\eta = 0.6$ is much more effective than at $\eta = 0$.

5. CONCLUSION

We theoretically investigated the performance of reservoir computing in a semiconductor laser with low-cut filtered optoelectronic feedback. The Santa Fe time-series prediction task was used for prediction of $n + 1$, $n + 2$ or $n + 3$ sampling point. The best NMSE value, in the order of 10^{-7} for $n + 1$ point prediction task, is obtained in the absence of feedback and rapid increase in NMSE is observed in the vicinity of Hopf bifurcation without regard to the feedback sign. On the contrary, the minimum values of NMSE for $n + 2$ and $n + 3$ point prediction task correspond to the Hopf bifurcation, and only for positive feedback.

REFERENCES

- [1] der Sande, G. V., Brunner, D., and Soriano, M. C., “Advances in photonic reservoir computing,” *Nanophotonics* **6**, 561–576 (jan 2017).
- [2] Brunner, D., Penkovsky, B., Marquez, B. A., Jacquot, M., Fischer, I., and Larger, L., “Tutorial: Photonic neural networks in delay systems,” *Journal of Applied Physics* **124**, 152004 (oct 2018).
- [3] Tanaka, G., Yamane, T., Héroux, J. B., Nakane, R., Kanazawa, N., Takeda, S., Numata, H., Nakano, D., and Hirose, A., “Recent advances in physical reservoir computing: A review,” *Neural Networks* **115**, 100–123 (jul 2019).
- [4] Andreas Weigend, N. G., [*Time Series Prediction*], Taylor & Francis Inc (1993).
- [5] Erneux, T. and Glorieux, P., [*Laser Dynamics*], Cambridge University Press (2009).
- [6] Kovalev, A. V., Islam, M. S., Locquet, A., Citrin, D. S., Viktorov, E. A., and Erneux, T., “Resonances between fundamental frequencies for lasers with large delayed feedbacks,” *Physical Review E* **99**, 062219 (jun 2019).

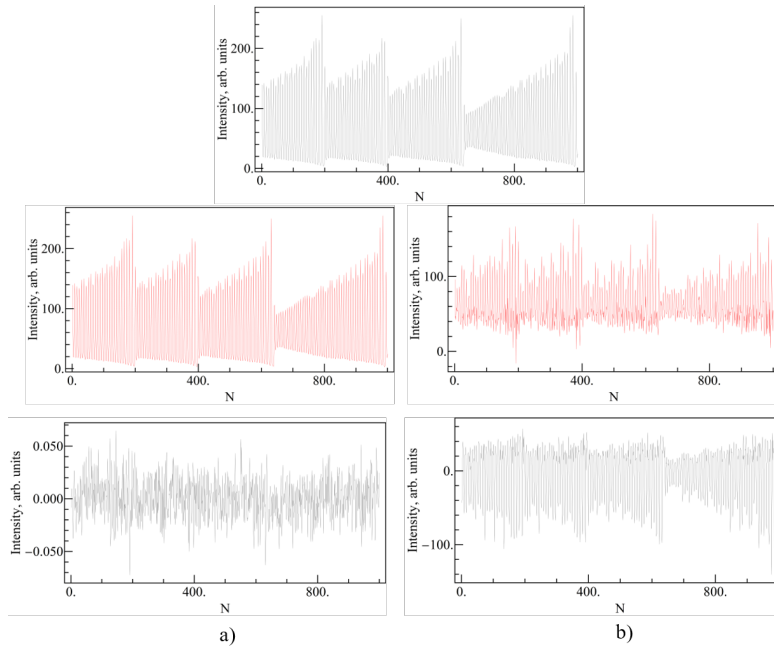


Figure 5. Temporal waveforms of the Santa Fe time-series prediction task using reservoir computing with 48 nodes. Input signal (black on top), predicted values (in red) in the absence of feedback $\eta = 0$ (a) and close to the bifurcation boundary $\eta = -0.6$ (b) and the difference in the initial and predicted values for those cases (black on bottom). The parameters are: $\varepsilon = 0.1, \tau = 1000, \tau_F = 2000, P = 0.26$.

- [7] Engelborghs, K., Luzyanina, T., and Roose, D., “Numerical bifurcation analysis of delay differential equations using DDE-BIFTOOL,” *ACM Transactions on Mathematical Software (TOMS)* **28**, 1–21 (mar 2002).